Homodimerization of Neurotensin 1 Receptor Involves Helices 1, 2, and 4: Insights from Quaternary Structure Predictions and Dimerization Free Energy Estimations

Daniele Casciari, Daniele Dell'Orco, and Francesca Fanelli*

Department of Chemistry and Dulbecco Telethon Institute (DTI), University of Modena e Reggio Emilia, Via Campi 183, 41100 Modena, Italy

Received February 12, 2008

A computational approach based upon rigid-body docking, ad hoc filtering, and cluster analysis has been combined with a protocol for dimerization free energy estimations to predict likely interfaces in the neurotensin 1 receptor (NTS1) homodimers. The results of this study suggest that the likely intermonomer interfaces compatible with in vitro binding affinity constants essentially involve helices 1, 2, and 4 and do not include disulfide bridges. The correlative model initially developed on Glycophorin A and herein extended to a G protein-Coupled Receptor (GPCR) appears to be a useful tool for estimating the association free energies of transmembrane proteins independent of the size and shape of the interface. In the desirable future cases, in which in vitro intermonomer binding affinities will be available for other GPCRs, such a correlative model will work as an additional criterion for helping in the selection of the most likely dimers.

INTRODUCTION

Increasing pieces of evidence indicate that G protein-Coupled Receptors (GPCRs) exist as homo- and heterodimers/oligomers in the cell membrane (reviewed in refs 1−9). A number of studies have shown that dimerization occurs early after biosynthesis, suggesting that it has a primary role in receptor maturation (reviewed in refs 7 and 8). For many GPCRs, oligomeric assembly has an important function in endoplasmic reticulum (ER) quality control because it masks specific retention signals or hydrophobic patches that would otherwise retain the proteins in ER.[10] Downstream signaling and regulatory processes, such as internalization, have also been shown to be influenced by the dimeric nature of the receptors (reviewed in refs 7 and 9). The question whether dimerization influences ligand-induced activation/regulation of GPCRs still remains to be answered. In fact, some studies suggest that ligand binding can regulate the dimer by either promoting or inhibiting its formation, whereas many others conclude that homodimerization and heterodimerization are constitutive processes that are not modulated by ligand binding (reviewed in ref 7). With respect to G protein coupling, increasing evidence from in vitro and in silico experiments on rhodopsin indicate that the monomeric form of the photoreceptor is able to fully activate the cognate G protein (transducin) or, in other words, that the complex between one rhodopsin molecule and heterotrimeric transducin is the functional unit.[11−16]

More or less resolved information on the receptor domains participating in the intermonomer interfaces in GPCR homodimers concerns a very limited number of systems, namely rhodopsin,[17,18] the β2-adrenergic receptor (β2-AR),[19,20] the D2-dopamine receptor (D2R),[21−23] and the 5-HT2C serotonin receptor.[24] With regard to rhodopsin, the geometrical constraints from AFM measurements drove the building of a semiempirical model of a higher order rhodopsin structure (PDB code: 1N3M).[17] According to this supramolecular model, two monomers of rhodopsin interact with each other at the extracellular (intradiscal) side (EL2, from both the monomers), at the cytoplasmic side (IL2 from both monomers), and also through Helices (H) 4 and 5. However, rhodopsin crystals obtained under different experimental conditions showed alternative dimeric architectures all compatible with the AFM images.[18] These dimers are characterized by H1−H1 or H8−H8 contacts.[18] With respect to the β2-AR, early in vitro experiments show that a peptide from H6 inhibited dimerization, suggesting that H6 is likely involved in intermonomer contacts.[19] Apparently in contrast with this evidence, crystal packing in the presence of cholesterol shows the significant involvement of such a hydrophobic molecule in the intermonomer interface.[20] In this framework, protein−protein contacts are minimal and include a pair of salt bridges between K60(1.59) (the numbering in parentheses follows the scheme proposed by Ballesteros and Weinstein,[25] where the first number indicates the helix and the numbers thereafter indicate the position of the helical residue relative to the most highly conserved residue within that helix, which is denoted as 50) and E338 from H8.[20] For the D2R, early in vitro experiments suggested the involvement of H6 and H7 in the intermonomer interface.[21] In contrast with these inferences, more recent evidence from cysteine cross-linking experiments suggested the involvement of H4 in the intermonomer interface. In fact, a cysteine from both monomers (C168(4.58) was found to be involved in an intermonomer disulfide bridge.[22] Very recent in vitro disulfide-trapping experiments on the 5-HT2C serotonin receptor suggest the existence of dimer architectures insensitive and sensitive to the functional state of the receptor.[24] In this respect, state-insensitive architectures would involve H1−H1 contacts, whereas state-sensitive architectures would be characterized by H4−H5 contacts.[24]

* Corresponding author phone: +39- 059-2055114; fax: +39- 059-373543; e-mail: fanelli@unimo.it.

10.1021/ci800048d CCC: $40.75
Published on Web 07/16/2008

Collectively, in vitro evidence seems to highlight different GPCR portions even for the same receptor as involved in intermonomer contacts.

The scarceness of data on the molecular architecture of GPCRs homodimers is accompanied by an almost total lack of quantitative data concerning the thermodynamics of GPCR dimerization. Unique, in this respect, is the neurotensin 1 receptor (NTS1), for which an estimate of the monomer−monomer binding affinity has been recently published.[26] Indeed, NTS1 dimerizes in detergent solution in a concentration-dependent manner, with an apparent affinity in the low nanomolar range.[26] This important information is, however, not complemented by the knowledge of the receptor domains involved in dimerization.

Recently, we have developed a computational procedure for predicting the supramolecular organization of transmembrane (TM) α-helical proteins by rigid-body docking.[27] Benchmarks of the approach were done on selected oligomers with known structure. In all the test cases, nativelike quaternary structures were predicted, i.e. characterized by a Root Mean Square Deviation of the α-carbon atoms (C_α-RMSDs) lower than 2.5 Å from the native oligomer.[27] The approach has been already employed for predicting likely interfaces in homodimers of the lutropin receptor (LHR), a member of Family A GPCRs.[28] We have also proposed a docking-based strategy to estimate mutational effects on the dimerization free energy of the TM helix of Glycophorin A (GpA).[29]

In this study, the two computational protocols have been combined in order to predict likely interfaces in NTS1 homodimers. For the first time, selection of the putative homodimer architecture has been based not only on the fulfillment of the membrane topology requirements and accomplishment of the shape complementarity but also on estimations of the dimerization free energy. The computational strategy presented in this study is transferable to all the members of Family A GPCRs.

METHODS

Comparative Modeling of NTS1. Comparative modeling of the NTS1 was carried out by means of the software MODELER 7v7,[30] by using the most complete and highest resolved structure of rhodopsin as a template (PDB code: 1U19).[31] The very recent release of the crystal structure of the human β2-AR[20,32] provided us with another potential template for modeling members of the rhodopsin family, including the NTS1. However, for NTS1, sequence similarity with rhodopsin is significantly higher than that with the β2-AR. In fact, the percentages of rhodopsin and β2-AR sequences identical to that of NTS1 are 23.6% and 19.6%, respectively. Thus, the photoreceptor is the proper template for comparative modeling of the NTS1.

All the receptor domains except for the N- and C-termini were modeled. The latter were excluded because of their low homology with the corresponding domains of rhodopsin and because they are unlikely to be involved in dimerization. The lack of homology between rhodopsin and NTS1 resides also in the third intracellular and extracellular loops (IL3 and EL3, respectively) as well as in the junctions between IL1 and H2 and between H4 and EL2. Problems related to the low homology in these domains were essentially faced through a de novo protocol for loop modeling implemented in MODELER[33] and by adding α-helix restraints to extend the termination of the helices connected with the low homologous loops. MODELER is, indeed, based upon the satisfaction of stereochemical restraints, which, for the homologous regions, are transferred from the template to the target protein, whereas, for the nonconserved portions, can be added by the user or computed following an energy-based de novo protocol. In this study, in order to define the proper lengths of the nonhomologous unstructured portions, eight different modifications of the rhodopsin template were probed, which were variably deleted at the following: a) the N-terminal half of H1, b) IL1, c) the N- and C-terminal ends of H2, d) the C-terminal end of H4 and the N-terminal end of EL2, e) IL3, and f) the extracellular ends of H6 and H7 as well as EL3. The eight different rhodopsin variances were employed as templates for comparative modeling of the target protein by using an equal number of sequence alignments. From each alignment, 200 receptor models were achieved by randomizing the Cartesian coordinates of the model. Randomizations produced 1600 models. Finally, the models resulting from four of the eight tested alignments revealed significantly higher quality than the rest. From each set of the 200 models derived from the best four alignments one model was selected, which was characterized by the highest 3D-Profile score (as computed within the QUANTA package) among the ten models characterized by the lowest restraint violations (i.e., the lowest MODELER Objective Function).

The results shown in this work refer to the alignment reported in Figure 1, by employing the rhodopsin template deprived of the 1−53, 68−71, 171−177, 227−242, 270−273, 278−291, and 224−348 amino acid stretches. In such a modified rhodopsin template, IL3 from the NTS1 sequence substitutes for that of the photoreceptor (sequence 227−242). Deletions of the beginning/ending of selected helices were instrumental in allowing one/two turn extensions of the helices itself and the proper connection with the de novo modeled portions of the loops. The rationale for probing one/two helix extensions is due to the demonstrated possibility that selected rhodopsin helices extend into the extracellular or intracellular environment, and significant differences in the length of a given helix can be observed depending on the crystallographic conditions.[34] As an example, in the 1GZM structure the cytosolic end of H5 is almost two turns longer than in the 1U19 structure.[31,35] The employment of such a modified form of the rhodopsin template was associated with the application of α-helix restraints to the 61−88, 97−104, 123−130, 200−212, 320−329, and 339−350 amino acid stretches of the target receptors (underlined sequences in Figure 1). These restraints were instrumental in modeling the first 19 amino acids of H1 as well as one- or two-turn elongations of the intracellular end of H2 and of the extracellular ends of H2, H4, H6 and H7 (Figure 1). The rationale for deleting the first 19 amino acids in H1 of rhodopsin is that P1.48 is present in rhodopsin but not in NTS1 (Figure 1). Therefore, we wanted to assess whether the absence of a proline at position 1.48 may cause a different tilt of H1 compared to rhodopsin, as suggested by the crystal structure of β2-AR that lacks P1.48 as well.

Different strategies were adopted to face problems due to lack of sequence similarity between template and target in selected protein portions. In detail: a) problems related to

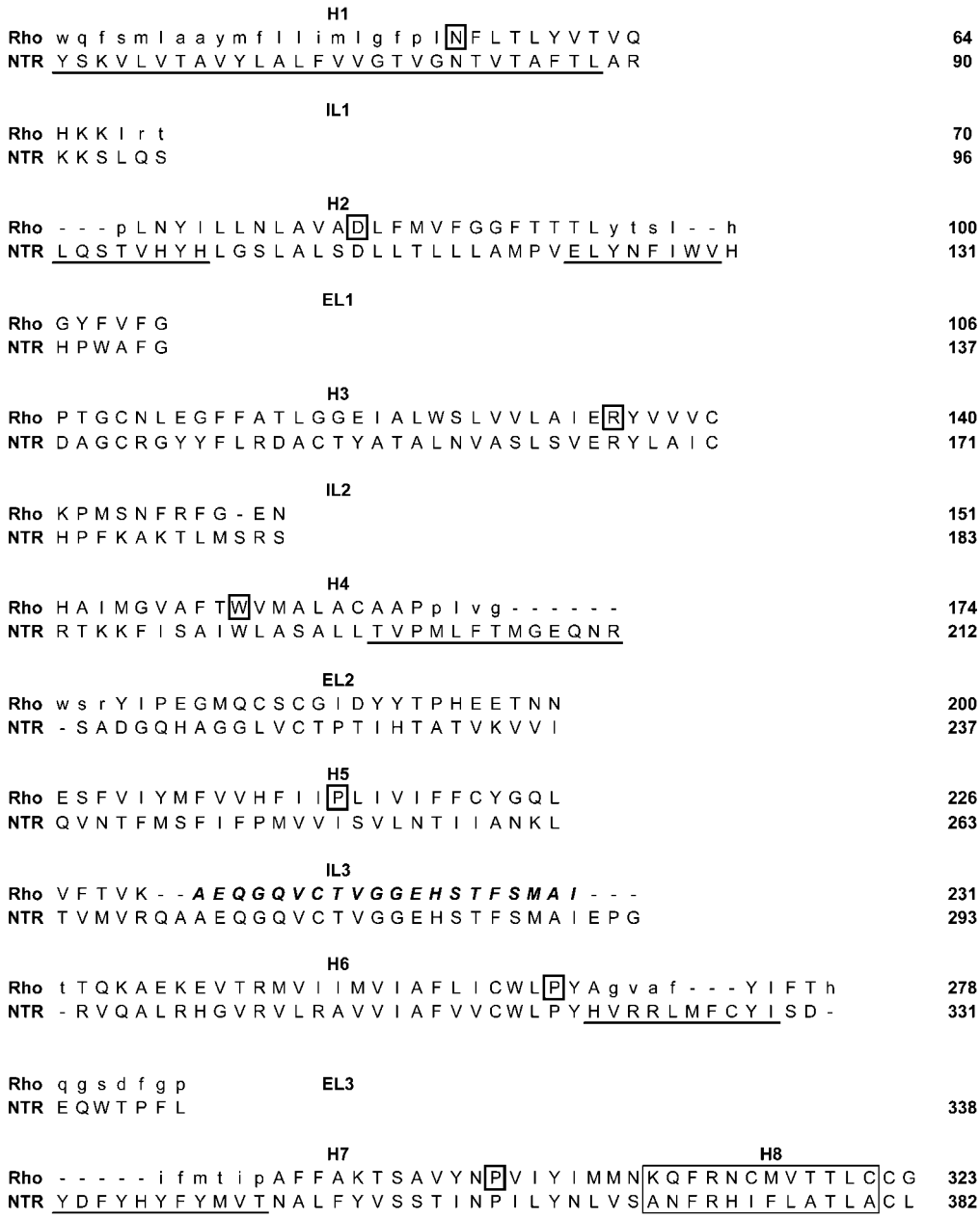

Figure 1. Sequence alignment between a modified form of bovine rhodopsin (PDB code: 1U19,[31] the template) and the human NTS1 (target) that was employed for comparative modeling. Rhodopsin is a chimera in which the IL3 from the NTS1 sequence (i.e., characters in italic bold) substitutes for the rhodopsin IL3 (the 227−242 sequence). The amino acid stretches 1−53, 68−71, 171−177, 227−242, 270−273, 278−291, and 224−348 were deleted from the 1U19 template (i.e., shown as lower case letters). The numbers concerning rhodopsin correspond to the ones in the photoreceptor sequence, independent of the substitution of the original IL3 with the one from the NTS1 sequence (that is ignored in the numbering) and independent of deletions. Underlined sequences in the target receptor (61−88, 97−104, 123−130, 200−212, 320−329, and 339−350) indicate the amino acids subjected to α-helical restraints during comparative modeling. The boxed amino acid in each rhodopsin helix corresponds to the amino acid no. 50 according to the Ballesteros and Weinstein nomenclature,[25] whereas the boxed amino acid stretch in both sequences at the end of H7 corresponds to H8.

the low homology in IL1/H2 junction were faced by de novo modeling[33] of the last three amino acids of the loop associated with one-turn extension of the N-term of H2. b) Problems due to the low sequence similarity at the H4/EL2 junction were faced by extending H4. c) With respect to IL3, this domain was separately built by using the segment 26−63 from the crystal structure of YbaB from *Haemophilus influenzae* (PDB code: 1J8B) as a template and then mounted into the rhodopsin template. The choice of the YbaB template was based upon predictions from the mGenThreader fold recognition server (http://bioinf.cs.ucl.ac.uk/psipred/psiform-.html). Finally, d) problems due to the lack of homology in EL3 were faced in the following way. The first three amino acids were modeled as extensions of H6, the seven central amino acids were built by an energy-based de novo protocol,[33] whereas the last five amino acids in this nonhomologous segment were modeled as extensions of the N-terminal end of H7 (Figure 1).

Molecular Dynamics Simulations. The four NTS1 models were subjected to automatic and manual rotation of the side-chain torsion angles when in nonallowed conformations as well as to energy minimization and MD simulations by using the GBSW implicit membrane-water model[36] implemented in CHARMM.[37] The all-hydrogen parameter set

PARAM22/CMAP was used. With respect to the physical parameters representing the membrane in the GBSW model, the surface tension coefficient (representing the nonpolar solvation energy) was set to 0.03 kcal/(mol·A^2). The membrane thickness centered at $Z=0$ was set to 30.0 Å with a membrane smoothing length of 5.0 Å ($w_m=2.5$ Å).

Minimizations were carried out by using 1500 steps of steepest descent followed by Adopted Basis Newton−Raphson (ABNR) minimization, until the root-mean-square gradient was less than 0.001 kcal/mol Å.

With respect to the setup of MD simulations, the lengths of the bonds involving the hydrogen atoms were restrained by the SHAKE algorithm, allowing for an integration time step of 0.001 ps during the heating, equilibration, and production phases. The systems were heated to 300 K with 7.5 K rises every 2.5 ps per 100 ps, by randomly assigning velocities from a Gaussian distribution. After heating, the system was allowed to equilibrate for 100 ps.

One disulfide bridge patch was applied to C141(3.25) and C224 (in EL2), homologous to the one in the rhodopsin structure.

The secondary structure of the helix bundle was preserved by assigning distance restraints (i.e., minimum and maximum allowed distances of 2.7 Å and 3.0 Å, respectively) between the backbone oxygen atom of residue i and the backbone nitrogen atom of residue i+4, except for prolines. The scaling factor of such restraints was 10, and the force constant at 300 K was 10 kcal/mol Å. The receptor amino acids present in noncanonical α-helical conformations in the input structure, a condition inherited from the rhodopsin template, were not subjected to any intrabackbone distance restraint. The selected intrahelix distance restraints were the outcome of short (100 ps) equilibrated MD trial runs, in which the beginning and ending of such restraints in each helix was varied. The selected computational setup and the input structure that produced the lowest deviation from the rhodopsin template, as far as the homologous domains are concerned, were employed to produce a 1 ns equilibrated trajectory. The structure averaged over the whole 1000 ps equilibrated trajectory was employed for docking simulation of dimerization.

Docking Simulations of NTS1 Dimerization. Predictions of NTS1 dimers were done by means of the rigid-body docking program ZDOCK 2.1.[38] The grid-based pairwise scoring function implemented in this version of the software accounts for shape and electrostatic complementarities neglecting the desolvation term, which is suitable for aqueous environments.[38] The Pairwise Shape Complementarity (PSC) scoring function is not explicitly based upon protein surface curvature or surface area, but it rather computes the total number of target-ligand atom pairs within a distance cutoff minus a clash penalty. Such procedure enhances pairwise target-ligand contacts and, by minimizing physical discontinuity, notably decreases the number of false positives in the docking output. The clash penalty instead accounts for potential bad contacts that may arise from the rigid-body approach. In detail, to account partially for different atom radii, the cutoff is defined as a parameter D plus the receptor atom radius. The unfavorable component of PSC is linearly proportional to the number of overlapping grid points between the receptor and the ligand.

For each protein system, a simulation run consisted of docking two identical copies of the monomer, i.e. one monomer was used as a fixed protein (target) and the other as a mobile protein (probe). The monomer employed both as a probe and a target was the NTS1 structure averaged over the whole 1 ns trajectory and minimized. A truncated form of such average was employed as well, which lacked IL3 (206−239 sequence, Figure 1).

A rotational sampling interval of 6° was employed, i.e. dense sampling, and the best 4000 solutions were retained and ranked according to the ZDOCK score (ZD-score). These solutions were subjected to a filter, the "membrane topology" filter, which discards all the solutions that violate the membrane topology requirements. In detail, the filter discards all the solutions characterized by a deviation angle from the original *z*-axis, tilt angle, and a displacement of the geometrical center along the *z*-axis, z-offset, above-defined threshold values. For the tilt angle and the z-offset, thresholds of 0.4 radians and 6.0 Å were, respectively, employed. The filtered solutions from each run were merged with the target protein, leading to an equivalent number of dimers that were subjected to cluster analysis. The C_α-RMSD threshold for each pair of superimposed dimers was set equal to 3.0 Å. All the amino acid residues in the dimer were included in C_α-RMSD calculations. Cluster analysis was based on the QT clustering algorithm[39] implemented in the FIPD software.[27] In this case study, the algorithm first calculated the C_α-RMSD for each superimposed pair of dimers/oligomers and then it computed the number of neighbors for each dimer/oligomer by using a threshold C_α-RMSD. The dimer/oligomer with the highest number of neighbors is considered as the center of the first cluster. All the neighbors of this configuration are removed from the ensemble of configurations to be counted only once. The center of the second cluster is then determined in the same way as for the first cluster, and this procedure is repeated until each structure is assigned to a cluster.

To identify the cluster of solutions with the best membrane topology, i.e. with the lowest values of both tilt angle and z-offset, we defined the MemTop index, $MemTop = \sqrt{\langle tilt_{nor}\rangle^2+\langle Z_{offnor}\rangle^2}$, were $\langle tilt_{nor}\rangle$ and $\langle Z_{offnor}\rangle$ are, respectively, the normalized tilt angle and the z-offset averaged over all the members of a given cluster. Normalization of each tilt angle and z-offset value was carried out by dividing each value for the respective cutoff value, i.e. 0.4 radians, for the tilt angle, and 6.0 Å, for the z-offset. The optimal value for such index is zero.

The predicted dimers were energy refined, following the same energy minimization setup as the one employed for the receptor monomer. The evaluation of the amino acid residues participating in the interface in the predicted dimers was based on the inter-residue interaction energy, computed as the difference between the total energy of an interface residue in the complex and the energy of that residue in the isolated monomer from the complex.

The buried interface surface in the predicted dimers was computed by means of the QUANTA package.

RESULTS

Structural Features of Wild Type NTS1. The first step in this study has been the building of a model of NTS1,

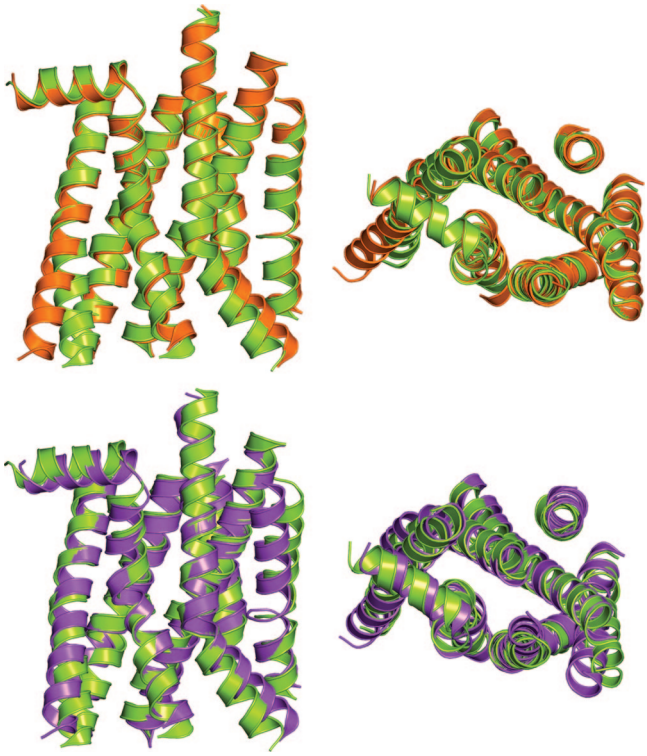

Figure 2. Superimposition between NTS1 and rhodopsin. Top: the superimposed structural models of rhodopsin (in green) and of the input structure of NTS1 (in orange) are shown seen in a direction parallel (left side) and perpendicular (right side) to the putative membrane surface. Bottom: the superimposed structural models of rhodopsin (in green) and of the average minimized structure of NTS1 (in violet) are shown seen in a direction parallel (left side) and perpendicular (right side) to the putative membrane surface. Superimpositions were carried out by fitting the main-chain atoms of the 35−64, 71−99, 107−140, 152−170, 202−226, 243−273, and 286−323 amino acid stretches of rhodopsin with those of the homologous segments in NTS1 (61−90, 100−128, 138−171, 1844−202, 239−263, 294−324, and 344−381). Only the regions found in α-helical conformation both in the crystal structure of rhodopsin and in the structural model of NTS1 are shown.

including all the domains except for the N- and C-termini. This was carried out through a corroborated approach consisting in comparative modeling followed by MD simulations.[40] The cornerstone of Family A of GPCRs, rhodopsin, has been employed as a template in comparative modeling, as it is the most adequate template available so far for NTS1. The NTS1 structural model employed as an input of MD simulations and the selected average minimized structure are characterized by main-chain RMSDs of 1.40 Å and 1.92 Å, respectively, from the crystal structure of rhodopsin. The RMSDs were computed by superimposing the main-chain atoms of the 35−64, 71−99, 107−140, 152−170, 202−226, 243−273, and 286−323 amino acid stretches, representing the α-helical segments of rhodopsin, with those of the homologous segments in NTS1 (61−90, 100−128, 138−171, 184−202, 239−263, 294−324, and 344−381). It is worth noting that the deviation between input NTS1 model and rhodopsin is entirely due to the different tilt of H1 and of the C-terminal end of H6 (Figure 2), whereas, in the case of the average minimized structure, it is more reliably distributed in all the matched segments, the largest deviations residing in H4 and H5 (Figure 2). The RMSD concerning the average minimized structure is close to the expected values according to the quantitative relation between the divergence of sequence and structure in proteins.[41] Indeed, considering the sequence identity of 21.8% between the matched segments of rhodopsin and NTS1, the expected RMSD values range between 1.5 Å and 2.2 Å. It is worth noting that the differences in the tilt of H1 between NTS1 and rhodopsin attenuate following MD simulations (Figure 2). This behavior, that is a common feature to all the average minimized structures derived from trial MD simulations, suggests that the lack of a proline at position 1.48 is somewhat compensated by another amino acid such as T1.47 that mimics the structural role of the rhodopsin's P1.48 (Figures 1 and 2). The β2-AR lacks both a proline at position 1.48 and a threonine at position 1.47. Thus, the peculiar tilt of H1 in the crystal structure of the β2-AR may be dictated, at least in part, by the lack of both P1.48 and of a α-helix breaker such as threonine or serine at positions 1.47 or 1.49 that could make a structural mimicry of the missing proline. The phenomenon of structural mimicry in GPCRs had been already postulated based upon the results of in vitro experiments and bioinformatics analyses.[42] An additional contribution to the peculiar tilt of H1 may come from packing interactions between H1 and H7 present in the β2-AR and not in rhodopsin or the NTS1 receptor.

Another case of structural mimicry between rhodopsin and NTS1 receptor occurs in H5 that in the crystal structure of rhodopsin holds a bulge due to both P5.50 and H5.46, which is involved in an interhelical interaction with E3.37. In the NTS1 receptor, the structural role of P5.50 and H5.46 are presumably mimicked, respectively, by S5.51 and P5.46 that interfere with the canonical network of intrabackbone H-bonds. The presence of such a structural mimicry is supported by the outcome of MD simulations that showed the maintenance of the bulge in H5 inherited from the rhodopsin template (Figure 2).

A number of intramolecular salt bridges characterize the selected average minimized structure of NTS1. Salt bridges in the extracellular domains include the following: a) D138(3.22)-R212, R142(3.26)-D215, and E209(3.66)-K234. The extracellular half of the seven-helix bundle includes the E123(2.61)-R148(3.32) and D149(3.33)-R323(6.55) salt bridges. Finally, in the cytosolic domains, salt bridges include E165(3.49)-R166(3.50), D291-R294(6.26), and E272-R303(6.35). The E165(3.49)-R166(3.50) interaction involves two members of the E/DRY highly conserved motif and is a feature inherited from the crystal structure of dark rhodopsin. This salt bridge has been postulated to stabilize the inactive state of the photoreceptor and of the homologous GPCRs, based upon the results of in vitro and in silico experiments.[40] The NTS1 lacks the glutamate at position 6.30, which contributes to stabilize the inactive state of rhodopsin through an interhelical salt bridge with the E/DRY arginine. This corroborates the hypothesis that, because of its lower conservation (32%) compared to the glutamate/aspartate at 3.49 (86%),[43] the role of the glutamate/aspartate at position 6.30 in maintaining the inactive receptor states, if any, is valid only for a very limited number of GPCRs.[40] Other structural features inherited from rhodopsin structure include the side-chain conformations and/or the interaction patterns of the highly conserved N81(1.50), D112(2.50), W170(4.50), and W316(6.48) as well as N360(7.49) and Y364(7.53). The last two amino acids belong to the NPxxY motif.

Table 1. Results of Docking Simulations for NTS1 Dimerization

clust. no.[a]	clust. pop.[b]	center[c]	$MemTop_{cent.}$[d]	$ZD_{cent.}$[e]	contacts[f]
1	12	152	1.020	15.86	H1−H2/H4
2	4	134	0.574	15.96	H4−H4
3	4	786	1.115	14.40	H4−H3/H4
4	3	512	1.265	14.84	H4−H2/H4
5	2	475	0.921	14.88	IL3/IL2
6	2	1391	0.767	13.90	H5−H1/H4
7	2	1606	0.901	13.76	H5−H4
8	2	1764	0.985	13.68	H4−H1/H8

[a] Cluster number; only solution clusters made of at least two solutions have been reported in this table. [b] Cluster population. [c] Rank number of the cluster center (i.e., the structure with the highest number of neighbors in a cluster). [d] MemTop index of the cluster center. [e] ZD-score of the cluster center. [f] Major receptor portions that participate in the interface.

Predictions of Intermonomer Interfaces. In this study, a computational approach based upon rigid-body docking, ad hoc filtering, automatic cluster analysis, and visual inspection of the cluster centers (the structure with the highest number of neighbors in a cluster) has been employed to predict likely interfaces in NTS1 homodimers. Simulations have been carried out on the minimized structure averaged over the whole 1 ns MD trajectory. A truncated form of such average lacking IL3 (206−239 sequence) has been considered as well, to assess the influence of IL3 on the outcome of docking simulations, as possible errors in the model are expected to reside in the structure of this receptor domain. Docking simulations on the full-length and truncated forms are overlapping. Therefore, the results shown herein will concern only the full-length NTS1 model.

The solutions that passed the membrane topology-based filter are 35 out of 4000 (Table 1). These solutions are distributed in eight clusters. The first cluster is more populated than the others (Table 1). A common feature to all the predicted interfaces is the involvement of H4; however, the best solutions are contained in the first two clusters (Table 1). In detail, the first cluster contains four solutions falling among the best 50 ones out of 4000, i.e. the solutions N. 18 (s18), s22, s32, and s35. The best topology (MemTop index equal to 0.890) is held by s32 that, therefore, is the selected solution from cluster 1. The best solution from cluster 2, s134, is worse than the best solution from cluster 1 in terms of ZD-score (17.48 for s32 and 15.96 for s134), but it is better in terms of the MemTop index. The latter is equal to 0.574, the lowest value among all the filtered solutions. We, therefore, have decided to select both s32 from cluster1 and s134 from cluster 2 as the best scored and most reliable docking solutions. The two predicted dimers, DIM1 for s32 and DIM2 for s134, have been subjected to slight manual adjustments to minimize the z-offset and to energy refinements. The buried surface at the monomer interface is 1745 Å^2 for DIM1 and 1065 Å^2 for DIM2, indicative of a greater interface in the former. DIM1 is, indeed, characterized by contacts between H1 and both H2 and H4 (and vice versa) as well as between EL1 from both dimers (Figure 3). In this dimer, van der Waals interactions between hydrophobic and aromatic amino acids are the essential components of the interface. In contrast, DIM2 is essentially characterized by H4−H4 and EL2-EL2 contacts (Figure 3). A greater number of positively and

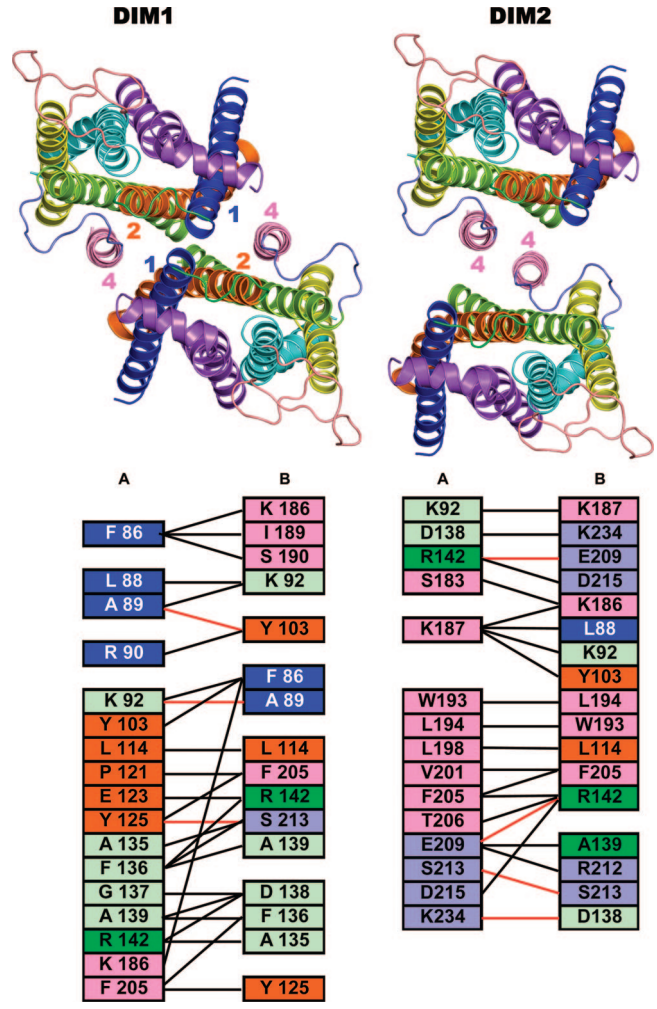

Figure 3. Top: Cartoon representation of two different dimeric models of the NTS1, seen from the intracellular side in a direction perpendicular to the membrane surface. The extracellular loops are not shown. H1, H2, H3, H4, H5, H6, and H7 are, respectively, colored in blue, orange, green, pink, yellow, cyan, and violet. H8 is colored in violet as well. IL1, IL2, and IL3 are respectively colored in lime, slate, and salmon. Only the helices participating in the intermonomer interfaces are indicated by numbers. Bottom: amino acids that contribute to the intermonomer interface. These amino acids, which are 33 for DIM1 and 32 for DIM2, have been selected for being involved in at least one intermonomer interaction with an energy below −1 kcal/mol. Squares are colored according to the amino acid location (see above in the legend). Light green and slate colors indicate EL1 and EL2, respectively. Black and red connecting lines indicate, respectively, interaction energies lower than −1 and −5 kcal/mol and comprise both side chain−side chain and side chain−backbone interactions. Drawings were done by means of the software PYMOL 0.97 (http://pymol.sourceforge.net/).

negatively charged amino acids from EL1, EL2 as well as the extracellular ends of H3 and H4, compared to DIM1, participate in the DIM2 interface. The latter is also characterized by the approaching of positively charged amino acids from both monomers. In fact, the positively charged nitrogen atom of K187, from monomer A, is respectively found at 4.2 Å and 3.5 Å, from the positively charged nitrogen atoms of K92 and K186, from monomer B.

Estimations of the Free Energy of Dimerization for DIM1 and DIM2. Very recently, we have presented a computational approach for estimating the effects of 32 single and double mutations on Glycophorin A (GpA) homodimer-

Table 2. In Vitro Binding Free Energy and Docking Scores for GpA

GpA variant[a]	$\Delta G°$ (kcal/mol)[b]	ZD_{best}[c]	ZD_w[d]
WT	−9.30	8.08	0.45
I77A	−9.20	8.48	0.47
F78A	−9.45	8.86	0.49
M81A	−9.45	8.48	0.47
G86A	−9.40	8.42	0.47
L75A	−8.20	8.08	0.45
G79A	−7.70	7.70	0.43
V80A	−8.90	8.40	0.47
G83A	−6.10	7.08	0.39
V84A	−8.30	8.24	0.46
T87A	−8.45	7.98	0.44
L75A/G79A	−7.00	7.26	0.40
L75A/V80A	−8.00	8.28	0.46
L75A/G83A	−5.70	6.96	0.39
G79A/V80A	−6.90	6.96	0.39
G79A/G83A	−5.70	6.80	0.38
G79A/V84A	−6.30	7.52	0.42
V80A/G83A	−5.80	6.30	0.35
G83A/V84A	−6.10	6.88	0.38
G79A/T87A	−6.50	7.66	0.43
G83A/T87A	−6.00	7.16	0.40

[a] Wild type and mutant GpA forms considered in the correlative model. [b] Absolute free energies of association derived by the experimental changes of binding free energy of GpA dimerization upon mutation, defined by the relationship: $\Delta\Delta G° = \Delta G°_{mut} - \Delta G°_{wt}$.[60–63] The $\Delta G°_{wt}$ (i.e., −9.3 kcal/mol) employed to derive $\Delta G°_{mut}$ was taken from ref 44. [c] ZD-score of the best solution over all the nativelike solutions from three independent docking runs. This value has been taken from ref 29. [d] Weighted ZD_{best}, obtained by dividing the original value for the number of amino acids at the interface in the native GpA dimer, i.e. 18.

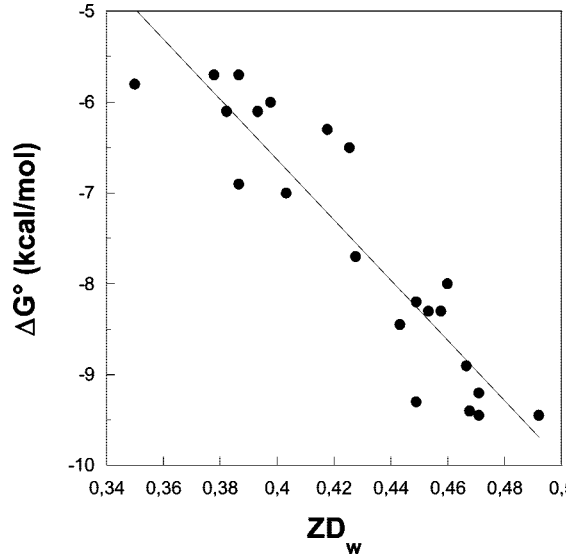

Figure 4. Linear trend between $\Delta G°$ and weighted ZD-score for the WT and 21 mutant forms of GpA. The linear correlation equation is as follows: $\Delta G° = 6.6(\pm 1.3) - 33.2(\pm 3.1)ZD_w$, $N = 22$, $\sigma = 0.55$, $R = 0.92$, $p < 0.0001$.This equation has been employed to estimate the dimerization free energy of the two predicted dimers of NTS1, i.e. DIM1 and DIM2. Prior to predictions, the ZD-scores of DIM1 and DIM2 (17.48 and 15.96, respectively) have been first divided for the respective number of interface amino acids (33 and 32, respectively), leading to the 0.530 and 0.499 values, respectively. The so weighted scores have, respectively, replaced the ZD_w variable in the above equation, leading to estimated $\Delta G°$ values of −11.0 and −10.0 kcal/mol.

ization.[29] Predictions were based on correlative models between relative binding free energy of helix-helix association (i.e., $\Delta\Delta G°$) and intermolecular interaction descriptors derived both by rigid-body docking and MD simulations. As for the ZDOCK-based correlative models, the computational index employed in the linear correlations was the ZD-score averaged over the nativelike solutions derived from three parallel docking runs. In order to make such correlative model applicable also to the predictive protocol employed in this study, which is based on a single docking run rather than on three parallel ones, for each nativelike GpA form, the best ZD-score (i.e., ZD_{best},Table 2) has been considered instead of an average score. In this case, we have selected the ZD-scores concerning the wild type (WT) and 21 mutant forms of GpA, which gave the best correlations with the absolute binding free energies. The latter have been derived from the $\Delta\Delta G°$ by employing the experimental $\Delta G°$ of the WT (−9.30 kcal/mol).[44] The absolute binding free energy gives a good correlation with ZD_{best}. In fact, the linear correlation equation is the following: $\Delta G° = (6.6 \pm 1.3) - (1.8 \pm 0.2)ZD_{best}$ ($N = 22$, $\sigma = 0.55$, $R = 0.92$, $p < 0.001$).

The interhelix interface in the native GpA dimer involves 18 amino acid residues, whereas the interfaces in the DIM1 and DIM2 predicted dimers of NTS1 involve 33 and 32 amino acids, respectively (Figure 3). These interface amino acids in DIM1 and DIM2 are those which are involved in at least one intermonomer interaction with an energy below −1.0 kcal/mol. These data are indicative of a more extended interface in the NTS1 dimers compared to GpA. Therefore, in order to make the correlative model obtained for GpA transferable to the NTS1 dimers, we have searched for a strategy to make the docking score independent of the extension of the interface. The most effective way, in this respect, turned out to be normalization of the ZD_{best} for the number of amino acids constituting the native interface in the GpA dimer. The linear trend obtained between the so weighted score (i.e., ZD_w, Table 2) and the association free energy is shown in Figure 4.

The relative linear correlation equation has been then employed to estimate the dimerization free energy of DIM1 and DIM2, the predicted dimers of NTS1. In this respect, the docking scores concerning DIM1 and DIM2 (17.48 and 15.96, respectively) have been first divided for the respective number of interface amino acids (33 and 32, respectively), leading to the 0.530 and 0.499 values, respectively. The estimated $\Delta G°$ values for DIM1 and DIM2 are −11.0 and −10.0 kcal/mol, respectively. The former shows a slightly better agreement with in vitro determinations that found a monomer−monomer K_d comprised between 2 nM and 20 nM (−10.5 kcal/mol < $\Delta G°$ < −12 kcal/mol (personal communication of Dr. Reinhard Grisshammer).[26]

DISCUSSION

To our knowledge, computational studies done so far to predict likely interfaces in GPCR dimers are very few and rely on sequence analyses.[45–50] In general, despite the demonstrated constitutive and functional importance of supramolecular assemblies of TM subunits or proteins, effective tools other than sequence-based methods for structure predictions of such assemblies are still lacking. Indeed, almost all the docking algorithms and approaches to quaternary structure predictions developed so far work with water-soluble proteins and most of them employ

geometrical constraints, including symmetry information.[51–56] The very few approaches intended for quaternary structure predictions of TM-helical proteins include a method based on Monte Carlo sampling of single TM helices.[57] The method is, however, limited to very simple homo-oligomers and requires knowledge about the oligomerization state of the protein, since symmetry information is used to filter the most realistic solutions. Another kind of information like the one inferred from cryo-electron microscopy and evolutionary data is, instead, employed by an alternative automated method for orienting TM helices.[58] Another docking method, GRAMM, deals with predictions of helix-helix packing interactions in water-soluble or TM-systems by employing geometrical criteria to discard false positives.[59]

Our computational approach to quaternary structure predictions of TM proteins is based upon rigid body docking simulations, membrane topology-based filtering, and cluster analysis.[27] It does not employ symmetry constraints either for improving sampling or in the filtering step. Furthermore, there are no size limitations in the systems under study, which are not limited to the TM domains but include also the water-soluble portions. Filtering is essential in discarding false positives, thus improving the predictive power of the protocol. Cluster analysis performed on the filtered solutions, which represent less than 4% of the total solutions provided by the docking program, is instrumental in individuating the nativelike solutions, which generally fall within the most populated clusters characterized by a good membrane topology (i.e., MemTop index preferably lower than 0.6) and within the top 50 solutions out of the 4000 collected. In most cases, they fall within the top ten.[27] Taken together, cluster population and docking score turned out to be effective criteria for detecting nativelike solutions.

In this study, the approach to quaternary structure predictions has been combined for the first time with a protocol recently developed for estimating mutational effects on the binding free energy of GpA homodimers.[29] The goal is to predict likely architectures in NTS1 homodimers. This has been made possible by the availability of in vitro determined intermonomer binding affinities, which represents a unique case within the rhodopsin family. The computational model of the receptor has been achieved by comparative modeling followed by MD simulations, according to a well established approach.[40] Binding affinity estimations have been done following an adjustment of the correlative model between ZD-score, that is essentially a size/shape descriptor, and free energy of GpA dimerization. This adjustment consists in dividing the ZD-score for the number of native interface residues and is instrumental in making the correlative model almost independent of the extension of the interface and, therefore, applicable to differently sized systems like GpA and GPCRs. The estimations of the NTS1 dimerization free energy carried out in this study have been essentially aimed at introducing an additional criterion to quaternary structure predictions. Primary criteria have been, indeed, the goodness of the membrane topology, as a reliability index, and the ZD-score, accounting for shape complementarity. The combinations between MemTop index and docking score has led to predictions of two possible architectures, DIM1 and DIM2, both characterized by the involvement of H4 in the interface (Figure 3). DIM1 fulfills better than DIM2 the criteria for solution selection previously inferred from benchmarks.[27] Indeed, this solution comes from the most populated cluster and falls within the top 50 solutions out of 4000. In contrast, DIM2 comes from the second most populated cluster and holds a rank number of 134. The reason why we chose also this solution was because it holds the lowest MemTop index among all the filtered solutions.

As expected, both dimers are characterized by the presence of hydrophobic amino acids in the TM portion of the interface, whereas salt bridges can be found between the extracellular end of H3 and EL1 in DIM1 or between EL1/extracellular end of H3 and EL2 in DIM2. The reliability of DIM2 is slightly undermined by the approaching of positively charged amino acids from both monomers. In line with a potentially higher reliability and greater interface of DIM1 compared to DIM2, the estimation of the intermonomer binding affinity seems to slightly privilege the former.

In conclusion, the results of this study provide insights into the features of the NTS1 homodimers suggesting that the likely interface compatible with in vitro binding affinity constants is essentially characterized by H1−H2/H4 contacts, which do not include disulfide bridges. This prediction should constitute the working hypothesis for in vitro experiments aimed at characterizing the interface in NTS1 homodimers and at providing in turn a validation for the computational approach.

The correlative model initially developed on GpA and herein extended to a GPCR appears to be an useful tool for estimating the association free energies of transmembrane proteins independent of the size and shape of the interface. Such a quantitative model for free energy estimations is, however, amenable to improvements following the availability of a significant set of thermodynamic and structural data for at least one GPCR. In the desirable future cases, in which in vitro intermonomer binding affinities will be available for other GPCRs, a robust correlative model between docking score and in vitro determined association free energy will work as an additional criterion for helping selection of the most likely dimers.

ACKNOWLEDGMENT

This study was supported by a Telethon-Italy grant no. S00068TELU.

REFERENCES AND NOTES

(1) Bouvier, M. Oligomerization of G-protein-coupled transmitter receptors. *Nat. Rev. Neurosci.* **2001**, *2*, 274–286.
(2) Milligan, G. Oligomerisation of G-protein-coupled receptors. *J. Cell. Sci.* **2001**, *114*, 1265–1271.
(3) Rios, C. D.; Jordan, B. A.; Gomes, I.; Devi, L. A. G-protein-coupled receptor dimerization: modulation of receptor function. *Pharmacol. Ther.* **2001**, *92*, 71–87.
(4) George, S. R.; O'Dowd, B. F.; Lee, S. P. G-protein-coupled receptor oligomerization and its potential for drug discovery. *Nat. Rev. Drug Discovery* **2002**, *1*, 808–820.
(5) Agnati, L. F.; Ferre, S.; Lluis, C.; Franco, R.; Fuxe, K. Molecular mechanisms and therapeutical implications of intramembrane receptor/receptor interactions among heptahelical receptors with examples from the striatopallidal GABA neurons. *Pharmacol. Rev.* **2003**, *55*, 509–550.
(6) Franco, R.; Canals, M.; Marcellino, D.; Ferre, S.; Agnati, L.; Mallol, J.; Casado, V.; Ciruela, F.; Fuxe, K.; Lluis, C.; Canela, E. I. Regulation of heptaspanning-membrane-receptor function by dimerization and clustering. *Trends Biochem. Sci.* **2003**, *28*, 238–243.
(7) Terrillon, S.; Bouvier, M. Roles of G-protein-coupled receptor dimerization. *EMBO Rep.* **2004**, *5*, 30–34.

(8) Bulenger, S.; Marullo, S.; Bouvier, M. Emerging role of homo- and heterodimerization in G-protein-coupled receptor biosynthesis and maturation. *Trends Pharmacol. Sci.* **2005**, *26*, 131–137.

(9) Maggio, R.; Novi, F.; Scarselli, M.; Corsini, G. U. The impact of G-protein-coupled receptor hetero-oligomerization on function and pharmacology. *Febs J.* **2005**, *272*, 2939–2946.

(10) Reddy, P. S.; Corley, R. B. Assembly, sorting, and exit of oligomeric proteins from the endoplasmic reticulum. *Bioessays* **1998**, *20*, 546–554.

(11) Jastrzebska, B.; Maeda, T.; Zhu, L.; Fotiadis, D.; Filipek, S.; Engel, A.; Stenkamp, R. E.; Palczewski, K. Functional characterization of rhodopsin monomers and dimers in detergents. *J. Biol. Chem.* **2004**, *279*, 54663–54675.

(12) Chabre, M.; le Maire, M. Monomeric G-Protein-Coupled Receptor as a Functional Unit. *Biochemistry* **2005**, *44*, 9395–9403.

(13) Ernst, O. P.; Gramse, V.; Kolbe, M.; Hofmann, K. P.; Heck, M. Monomeric G protein-coupled receptor rhodopsin in solution activates its G protein transducin at the diffusion limit. *Proc. Natl. Acad. Sci. U.S.A.* **2007**, *104*, 10859–10864.

(14) Bayburt, T. H.; Leitz, A. J.; Xie, G.; Oprian, D. D.; Sligar, S. G. Transducin activation by nanoscale lipid bilayers containing one and two rhodopsins. *J. Biol. Chem.* **2007**, *282*, 14875–14881.

(15) Whorton, M. R.; Jastrzebska, B.; Park, P. S.; Fotiadis, D.; Engel, A.; Palczewski, K.; Sunahara, R. K. Efficient coupling of transducin to monomeric rhodopsin in a phospholipid bilayer. *J. Biol. Chem.* **2007**,

(16) Dell'Orco, D.; Seeber, M.; Fanelli, F. Monomeric dark rhodopsin holds the molecular determinants for transducin recognition: insights from computational analysis. *FEBS Lett.* **2007**, *581*, 944–948.

(17) Liang, Y.; Fotiadis, D.; Filipek, S.; Saperstein, D. A.; Palczewski, K.; Engel, A. Organization of the G protein-coupled receptors rhodopsin and opsin in native membranes. *J. Biol. Chem.* **2003**, *278*, 21655–21662.

(18) Lodowski, D. T.; Salom, D.; Le Trong, I.; Teller, D. C.; Ballesteros, J. A.; Palczewski, K.; Stenkamp, R. E. Crystal packing analysis of Rhodopsin crystals. *J. Struct. Biol.* **2007**, *158*, 455–462.

(19) Hebert, T. E.; Moffett, S.; Morello, J. P.; Loisel, T. P.; Bichet, D. G.; Barret, C.; Bouvier, M. A peptide derived from a beta2-adrenergic receptor transmembrane domain inhibits both receptor dimerization and activation. *J. Biol. Chem.* **1996**, *271*, 16384–16392.

(20) Cherezov, V.; Rosenbaum, D. M.; Hanson, M. A.; Rasmussen, S. G.; Thian, F. S.; Kobilka, T. S.; Choi, H. J.; Kuhn, P.; Weis, W. I.; Kobilka, B. K.; Stevens, R. C. High-resolution crystal structure of an engineered human beta2-adrenergic G protein-coupled receptor. *Science* **2007**, *318*, 1258–1265.

(21) Ng, G. Y.; O'Dowd, B. F.; Lee, S. P.; Chung, H. T.; Brann, M. R.; Seeman, P.; George, S. R. Dopamine D2 receptor dimers and receptor-blocking peptides. *Biochem. Biophys. Res. Commun.* **1996**, *227*, 200–204.

(22) Guo, W.; Shi, L.; Javitch, J. A. The fourth transmembrane segment forms the interface of the dopamine D2 receptor homodimer. *J. Biol. Chem.* **2003**, *278*, 4385–4388.

(23) Guo, W.; Filizola, M.; Weinstein, H.; Javitch, J. A. Crosstalk in G protein-coupled receptors: Changes at the transmembrane homodimer interface determine activation. *Proc. Natl. Acad. Sci. U.S.A.* **2005**, *102*, 17495–17500.

(24) Mancia, F.; Assur, Z.; Herman, A. G.; Siegel, R.; Hendrickson, W. A. Ligand sensitivity in dimeric associations of the serotonin 5HT2c receptor. *EMBO Rep.* **2008**, *9*, 363–369.

(25) Ballesteros, J. A.; Weinstein, H. Integrated methods for the construction of three-dimensional models and computational probing of structure-function relations in G protein-coupled receptors. *Methods Neurosci.* **1995**, *25*, 366–428.

(26) White, J. F.; Grodnitzky, J.; Louis, J. M.; Trinh, L. B.; Shiloach, J.; Gutierrez, J.; Northup, J. K.; Grisshammer, R. Dimerization of the class A G protein-coupled neurotensin receptor NTS1 alters G protein interaction. *Proc. Natl. Acad. Sci. U.S.A.* **2007**, *104*, 12199–12204.

(27) Casciari, D.; Seeber, M.; Fanelli, F. Quaternary structure predictions of transmembrane proteins starting from the monomer: a docking-based approach. *BMC Bioinformatics* **2006**, *7*, 340.

(28) Fanelli, F. Dimerization of the lutropin receptor: insights from computational modeling. *Mol. Cell. Endocrinol.* **2007**, *260*−*262*, 59–64.

(29) Dell'Orco, D.; De Benedetti, P. G.; Fanelli, F. In silico screening of mutational effects on transmembrane helix dimerization: insights from rigid-body docking and molecular dynamics simulations. *J. Phys. Chem. B* **2007**, *111*, 9114–9124.

(30) Sali, A.; Blundell, T. L. Comparative protein modelling by satisfaction of spatial restraints. *J. Mol. Biol.* **1993**, *234*, 779–815.

(31) Okada, T.; Sugihara, M.; Bondar, A. N.; Elstner, M.; Entel, P.; Buss, V. The retinal conformation and its environment in rhodopsin in light of a new 2.2 A crystal structure. *J. Mol. Biol.* **2004**, *342*, 571–583.

(32) Rosenbaum, D. M.; Cherezov, V.; Hanson, M. A.; Rasmussen, S. G.; Thian, F. S.; Kobilka, T. S.; Choi, H. J.; Yao, X. J.; Weis, W. I.; Stevens, R. C.; Kobilka, B. K. GPCR engineering yields high-resolution structural insights into beta2-adrenergic receptor function. *Science* **2007**, *318*, 1266–1273.

(33) Fiser, A.; Do, R. K.; Sali, A. Modeling of loops in protein structures. *Protein Sci.* **2000**, *9*, 1753–1773.

(34) Palczewski, K. G protein-coupled receptor rhodopsin. *Annu. Rev. Biochem.* **2006**, *75*, 743–767.

(35) Li, J.; Edwards, P. C.; Burghammer, M.; Villa, C.; Schertler, G. F. Structure of bovine rhodopsin in a trigonal crystal form. *J. Mol. Biol.* **2004**, *343*, 1409–1438.

(36) Im, W.; Feig, M.; Brooks, C. L.,, III. An implicit membrane generalized born theory for the study of structure, stability, and interactions of membrane proteins. *Biophys. J.* **2003**, *85*, 2900–2918.

(37) Brooks, B. R.; Bruccoleri, R. E.; Olafson, B. D.; States, D. J.; Swaminathan, S.; Karplus, M. Charmm: a program for macromolecular energy, minimization and dynamics calculations. *J. Comput. Chem.* **1983**, *4*, 187–217.

(38) Chen, R.; Weng, Z. A novel shape complementarity scoring function for protein-protein docking. *Proteins* **2003**, *51*, 397–408.

(39) Heyer, L. J.; Kruglyak, S.; Yooseph, S. Exploring expression data: identification and analysis of coexpressed genes. *Genome Res.* **1999**, *9*, 1106–1115.

(40) Fanelli, F.; De Benedetti, P. G. Computational modeling approaches to Structure-Function Analysis of G Protein-Coupled Receptors. *Chem. Rev.* **2005**, *105*, 3297–3351.

(41) Chothia, C.; Lesk, A. M. The relation between the divergence of sequence and structure in proteins. *Embo J.* **1986**, *5*, 823–826.

(42) Ballesteros, J. A.; Shi, L.; Javitch, J. A. Structural mimicry in G protein-coupled receptors: implications of the high-resolution structure of rhodopsin for structure-function analysis of rhodopsin-like receptors. *Mol. Pharmacol.* **2001**, *60*, 1–19.

(43) Mirzadegan, T.; Benko, G.; Filipek, S.; Palczewski, K. Sequence analyses of G-protein-coupled receptors: similarities to rhodopsin. *Biochemistry* **2003**, *42*, 2759–2767.

(44) Fleming, K. G.; Ren, C. C.; Doura, A. K.; Eisley, M. E.; Kobus, F. J.; Stanley, A. M. Thermodynamics of glycophorin A transmembrane helix dimerization in C14 betaine micelles. *Biophys. Chem.* **2004**, *108*, 43–49.

(45) Gouldson, P. R.; Bywater, R. P.; Reynolds, C. A. Correlated mutations amongst the external residues of G-protein coupled receptors. *Biochem. Soc. Trans.* **1997**, *25*, 529S.

(46) Gouldson, P. R.; Snell, C. R.; Bywater, R. P.; Higgs, C.; Reynolds, C. A. Domain swapping in G-protein coupled receptor dimers. *Protein Eng.* **1998**, *11*, 1181–1193.

(47) Gouldson, P. R.; Higgs, C.; Smith, R. E.; Dean, M. K.; Gkoutos, G. V.; Reynolds, C. A. Dimerization and domain swapping in G-protein-coupled receptors: a computational study. *Neuropsychopharmacology* **2000**, *23*, S60−77.

(48) Dean, M. K.; Higgs, C.; Smith, R. E.; Bywater, R. P.; Snell, C. R.; Scott, P. D.; Upton, G. J.; Howe, T. J.; Reynolds, C. A. Dimerization of G-protein-coupled receptors. *J. Med. Chem.* **2001**, *44*, 4595–4614.

(49) Filizola, M.; Olmea, O.; Weinstein, H. Prediction of heterodimerization interfaces of G-protein coupled receptors with a new subtractive correlated mutation method. *Protein Eng.* **2002**, *15*, 881–885.

(50) Filizola, M.; Weinstein, H. Structural models for dimerization of G-protein coupled receptors: the opioid receptor homodimers. *Biopolymers* **2002**, *66*, 317–325.

(51) Eisenstein, M.; Shariv, I.; Koren2, G.; Friesem, A. A.; Katchalski-KatziR, E. Modeling Supra-molecular Helices: Extension of the Molecular Surface Recognition Algorithm and Application to the Protein Coat of the Tobacco Mosaic Virus. *J. Mol. Biol.* **1997**, *266*, 135–143.

(52) Gardiner, E. J.; Willett, P.; Artymiuk, P. J. Protein Docking Using a Genetic Algorithm. *Proteins* **2001**, *44*, 44–56.

(53) Berchanski, A.; Eisenstein, M. Construction of Molecular Assemblies via Docking: Modeling of Tetramers with D2 Symmetry. *Proteins* **2003**, *53*, 817–829.

(54) Inbar, Y.; Benyamini, H.; Nussinov, R.; Wolfson, H. J. Protein structure prediction via combinatorial assembly of sub-structural units. *Bioinformatics* **2003**, *19*, i158–i168.

(55) Berchanski, A.; Segal, D.; Eisenstein, M. Modeling Oligomers with Cn or Dn Symmetry: Application to CAPRI Target 10. *Proteins* **2005**, *60*, 202–206.

(56) Pierce, B.; Tong, W.; Weng, Z. M-ZDOCK: a grid-based approach for Cn symmetric multimer docking. *Bioinformatics* **2005**, *21*, 1472–1478.

(57) Kim, S.; Chamberlain, A. K.; Bowie, J. U. A simple method for modeling transmembrane helix oligomers. *J. Mol. Biol.* **2003**, *329*, 831–840.

(58) Fleishman, S. J.; Harrington, S.; Friesner, R. A.; Honig, B.; Ben-Tal, N. An Automatic Method for Predicting Transmembrane Protein Structures Using Cryo-EM and Evolutionary Data. *Biophys. J.* **2004**, *87*, 3448–3459.

(59) Vakser, I. A.; Jiang, S. Strategies for modeling the interactions of transmembrane helices of G protein-coupled receptors by geometric complementarity using the GRAMM computer algorithm. *Methods Enzymol.* **2002**, *343*, 313–328.

(60) Doura, A. K.; Fleming, K. G. Complex interactions at the helix-helix interface stabilize the glycophorin A transmembrane dimer. *J. Mol. Biol.* **2004**, *343*, 1487–1497.

(61) Doura, A. K.; Kobus, F. J.; Dubrovsky, L.; Hibbard, E.; Fleming, K. G. Sequence context modulates the stability of a GxxxG-mediated transmembrane helix-helix dimer. *J. Mol. Biol.* **2004**, *341*, 991–998.

(62) Fleming, K. G.; Ackerman, A. L.; Engelman, D. M. The effect of point mutations on the free energy of transmembrane α helix dimerization. *J. Mol. Biol.* **1997**, *272*, 266–275.

(63) Fleming, K. G.; Engelman, D. M. Specificity in transmembrane helix-helix interactions can define a hierarchy of stability for sequence variants. *Proc. Natl. Acad. Sci. U.S.A.* **2001**, *98*, 14340–14344.

CI800048D